Spatial Resolution of Immune Cell Lineages in the Tumor Microenvironment of Plasma Cell Dyscrasias

AACR Poster #11

Medbh A. Dillon[1]**, Lisa Arvidson[2]**, Cole G. Phalen[1], Ruoxin Li[1], Imran McGrath[1], Julian R. Ishibashi[1], John B. Johanneson[1], Kevin J. Li[1], Zachary J. Thomson[1], Samuel Jensen[2], Jocelin Malone[1], Mackenzie S. Kopp[1], Susan A. Lundmann[1], Adam K. Savage[1], Claire E. Gustafson[1], Marla Glass[1], Emma L. Kuan[1], Lucas T. Graybuck[1], Xiao-jun Li[1], Troy R. Torgerson[1], Peter J. Skene[1], Stephanie Añover-Sombke[1], Melinda L. Angus-Hill[1]

*[1]Allen Institute for Immunology, Seattle, WA. [2]Cell Signaling Technology, Danvers, MA, **These authors contributed equally*

ABSTRACT

Plasma cell dyscrasias (PCDs) are diseases of the hematologic system, with Multiple Myeloma (MM) as the most common disease. Less common PCDs include primary and secondary extramedullary plasmacytomas (EMP), which occur in soft tissues. EMPs are typically solitary and infrequent, often localized in the upper aerodigestive and gastrointestinal tracts, lung, and lymph nodes among other organs, and can convert to Multiple Myeloma. Secondary extramedullary plasmacytomas are often noted in advanced disease following multiple rounds of therapy and are commonly associated with poor prognosis. Studies aimed at gaining a better understanding of soft tissue EMPs, whether solitary plasmacytomas with undiagnosed multiple myeloma or in the context of recurrent or metastatic EMP disease, are limited. In this study, we employ a comprehensive approach using multiple modalities, including dissociated CITE-seq, spatial transcriptomics, and multiplexed spatial immuno-fluorescence imaging to interrogate the tumor and immune landscape in EMP disease. Importantly, the use of the same biomarker antibodies across these modalities provides a cross-data-framework for a deep contextual understanding of the immune and tumor cell organization and cell-to-cell signaling in EMP. Ultimately, this study provides new insights into patient-to-patient and tumor location variability, tumor and immune cell microenvironment heterogeneity, and possible future therapeutic strategies for EMP.

INTRODUCTION

Single-cell technologies are invaluable for analyzing the cellular and molecular aspects of tumor cells and their environment. Integrating spatial transcriptomics and proteomics with single-cell analysis boosts our comprehension of tumor heterogeneity and the complex interplay between tumor cells and immune system evasion. This method is key to deepening our understanding of tumor biology and the mechanisms of immune escape.

The bone marrow environment consists of various cellular compartments including mesenchymal stromal cells, immune cells, endothelial cells, adipocytes, osteoclasts, and osteoblasts. Clarifying the complexities of the bone marrow niche, and its role in the progression of multiple myeloma (MM), including aspects of immune evasion, is still a work in progress

Moreover, the persistent clonal and subclonal evolution of the cancer, along with changes in the environment leading to relapse, underscores the importance of a multifaceted approach to understanding MM. This approach should explore changes in the immune system and microenvironment within the tissue to better identify new strategies for targeting tumor clones that manage to evade the immune system and treatment.

In this study, we adopt a multi-modal strategy to begin unraveling the intricacies of multiple myeloma (MM) and its interactions within the immune and tissue microenvironments. Utilizing minimal tissue from archival samples, we have implemented a range of techniques including spatial transcriptomics (probe-based panel and whole transcriptome), single-cell transcriptomics, and spatial proteomics, unified by a consistent use of antibodies across these technologies. Through this comprehensive analysis, we've pinpointed distinct cell types grouped into separate clusters. These clusters share common biomarkers, yet they exhibit a rich diversity in functional pathways, highlighting the complex interplay within the MM microenvironment.

METHODS

- **FFPE Sample Collection:** Samples of multiple myeloma, normal donor bone marrow biopsies, and plasmacytoma were sourced from Accio Biosciences or acquired via collaboration with the OHSU Biolibrary.
- **Tissue Preparation:** Serial sections (5 µm) or scrolls (25 µm) underwent processing with Xenium or Visium following manufacturer protocols (Figure 1A). This included the integration of bridging antibodies, conjugated with ADT oligos, provided by Cell Signaling Technology.
- **Single Cell Dissociation and CITEseq:** Executed according to MACSima (Miltenyi) and 10X Genomics guidelines. Modifications included antigen retrieval, tissue fixation, and the addition of CST bridging antibodies.
- **Ground Truth Assessment:** A serial section served as a "ground truth" control, probed with custom fluorophore-conjugated CST bridging antibodies to establish a baseline for cross-platform comparison.
- **Data Collection and Analysis:**
  - Cell DIVE data underwent segmentation and analysis using Aivia software (Leica Microsystems).
  - HALO software (Indica Labs) facilitated image overlays in Figure 1D.
  - Analysis of Xenium, Visium, and scCITE-seq data employed 10X Genomics software (Ref. 1) and Python packages Scanpy and Squidpy for integrative cross-platform analysis.

RESULTS

Figure 1:

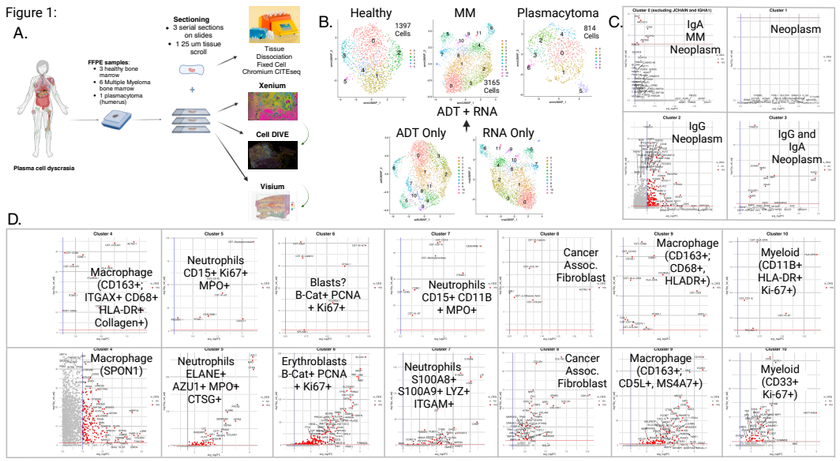

Figure 1: Layout and Initial Results from scFFPE CITE-seq Experiments on Bone Marrow Biopsies(A) This panel presents the experimental setup used in the study. **(B)** We performed the single cell FFPE CITE-seq (scFFPE CITE-seq) experiment on biopsies from normal bone marrow, as well as from bone marrow affected by multiple myeloma (MM) and plasmacytoma. The analysis involved clustering cells and performing dimensionality reduction in UMAP space based on antibody-derived tags (ADT), RNA, or a combination of RNA + ADT. **(C)** In the case of MM, ADTs were not effective in distinguishing markers of malignant plasma cells across different patients. Conversely, RNA probes were capable of identifying differentially expressed genes within these cell clusters. **(D)** Across both ADT and RNA-based clusters, additional cell types were consistently annotated, highlighting commonalities in cell type identification regardless of the clustering method used.

Figure 2:

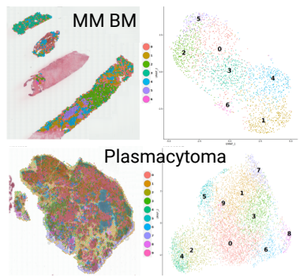

Figure 2: Visium Analysis with CST_Bridge ADT Enhancement. This figure showcases representative data from Visium analysis, incorporating CST_Bridge ADT enhancement. The results display cellular clustering and dimensionality reduction (UMAP) similar to those observed with single-cell tissue dissociation CITEseq, underscoring the comparative effectiveness of this method in analyzing cellular compositions.

Figure 3: Integrating Single Cell and Spatial Data across Xenium, Visium, and Cell DIVE

Using the Xenium multi-tissue and cancer panel, sections were probed and data individually analyzed, then phenotypically merged into a single dataset. After harmonizing data across patients, scRNAseq data underwent Leiden clustering and UMAP generation (A). Most cell cluster types remained consistent across platforms, with cancer-associated fibroblasts noted in scCITEseq, and adipocytes and endothelial cells predominantly identified in Xenium (B, see also Fig. 1 D). All clusters were consistently found in all Multiple Myeloma samples (C). Cytotoxic T cell DEGs from cluster 10 were identified on Visium and further detailed on Cell DIVE (D).

Figure 4: Bridging Single Cell and Spatial Data through Deconvolution Techniques

This figure focuses on bridging single-cell and spatial data via deconvolution of Visium data single cell dissociated FFPE CITE-seq, (scFFPE CITE-seq) Post-deconvolution, scFFPE CITEseq cluster expression was mapped onto Visium data (A,D). Visium, not providing single-cell resolution, showed bright red for dominant cell type areas matching scFFPE CITE-seq clusters. A yellow-to-green gradient indicated the presence of multiple cell types alongside the primary one, with grey indicating no DEG overlap with Visium data. The deconvolved Visium data's alignment with RNA and ADT from scRNAseq data revealed neutrophil specific markers in Cluster 5 (B,C) and cancer fibroblast specific markers in Cluster 6 (E,F), highlighting the precision of RNA and barcoded ADT in cell characterization.

Figure 3:

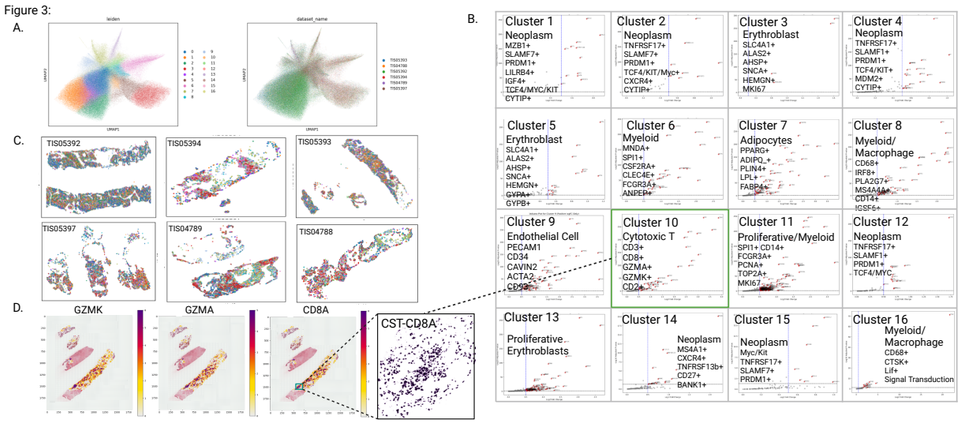

Figure 4:

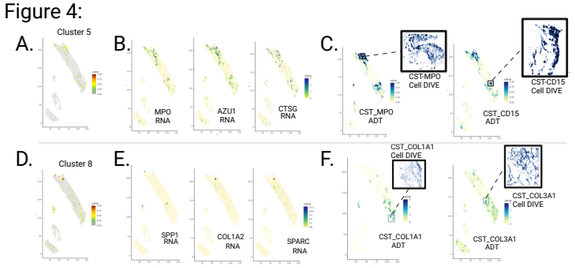

Figure 5:

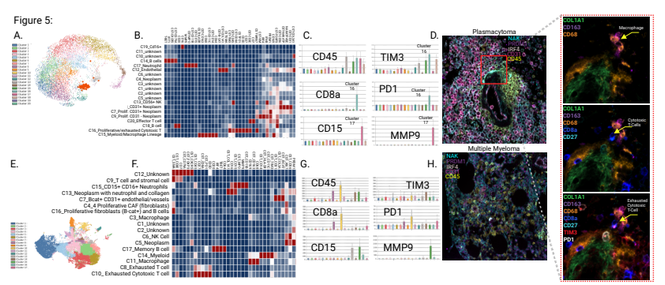

Figure 5 Legend: Cell DIVE imaging and Data Analysis of over 40 Biomarkers. (A & B) Cells were segmented using DapI and multiple membrane markers, clustered by K-means, and visualized in UMAP for spatial representation. **(B & F)** Dendrograms show relative biomarker intensities across clusters, highlighting expression variations.**(C & D)** T cell exhaustion and neutrophil contribution were analyzed across clusters, and validated by manual examination.

RESULTS AND CONCLUSIONS

To address the gap in single-cell data for both healthy and diseased bone marrow tissue, especially in multiple myeloma (MM), we developed a comprehensive single-cell dataset utilizing FFPE dissociation and scCITE-seq (scFFPE CITE-seq). Enhancing our methodology, we engineered and validated 30 antibodies for FFPE tissues, which were conjugated to ADT and fluorophores for broad platform compatibility. Despite the complexities of bone marrow dissociation and working with FFPE blocks over 10 years old, we successfully sequenced cells from both healthy donors and MM patients, including a secondary Plasmacytoma case (Figure 1B). Employing Leiden clustering and differential gene expression analysis, we categorized numerous cell types (Figure 1), notably identifying malignant cells with plasma cell markers in MM samples. These cells were grouped by non-immunoglobulin genes, following the strategic removal of immunoglobulins before clustering (Figure 1C). This investigation confirmed the dual utility of RNA and ADT antibodies in pinpointing specific cell type biomarkers, with ADTs significantly enhancing cell type identification over RNA analysis (Figure 1D). Our analysis revealed patterns corresponding to macrophages, neutrophils, myeloid cells, erythroblasts, and cancer-associated fibroblasts within the clusters, offering insights into the bone marrow microenvironment's transcriptional dynamics and the complex interplay of cellular states in MM.

Visium provides a whole transcriptome-probe based spatial profiling platform that, despite its inability to offer single-cell resolution, facilitates deep sequencing and spatial transcriptome analysis (Figure 2). Xenium analysis, using the Xenium multi-tissue and cancer panel, which includes 377 probes, on a serial tissue section, allowed us to explore MM at a nuanced level, revealing differential expression of cell type biomarkers across clusters and identifying six distinct malignant clusters as well as erythroblast, myeloid, adipocyte, myeloid/macrophage, endothelial, and cytotoxic T cells (Figure 3A, B). Interestingly, lack of tissue dissociation effects on the Xenium platform led to the identification of endothelial cells and adipocytes (Figure 3 B), while cancer-associated fibroblasts were uniquely detected in dissociated tissue (Figure 1 C). These clusters, once mapped onto the tissue, provided a window into the spatial interactions between cells within each cluster (Figure 3C). Further cross-platform analysis showed Xenium's Cluster 10, marked as CD8+ cytotoxic T cells, aligned onto Visium data for CD8 and additional markers. Validation through a bridge antibody in Cell DIVE confirmed robust CD8 staining in the same region (Figure 3D, Boxed inset), demonstrating the effectiveness of integrating diverse spatial and single-cell technologies for a richer understanding of tissue microenvironments and cellular interactions in cancer pathology.

To circumvent its single-cell resolution limitation, and to delve deeper into tissue-wide cellular diversity via Visium, we employed deconvolution with scFFPE CITE-seq data and bridge ADT for precise cell identification. Mapping of Clusters 5 and 8 onto Visium data (Figure 1D) uncovered spatially distinct areas predominantly occupied by Cancer-Associated Fibroblasts (CAFs) and neutrophils (Figure 4 A, D). Specific RNAs (Figure 4 B, E) and ADTs (Figure 4 C, F) from these clusters, when mapped, exhibited distinct patterns, further accentuated by ADT use, and corroborated using fluorophore-conjugated antibodies on Cell DIVE (see boxed insets on (Figure 4 C, F).

For validating our hypotheses and establishing a benchmark, we applied bridging antibodies to stain consecutive sections of both healthy and MM bone marrow, as well as plasmacytoma samples using Cell DIVE. Like with the other methods, this process, followed by segmentation, clustering, UMAP creation, and dendrogram analysis, allowed for the basic categorization of cell types (Figure 5 A, B, E, F). Notably, our analysis identified CD8+ cytotoxic T cells in plasmacytoma samples prominently expressing both TIM3 and PD1, suggesting an exhausted phenotype (Figure 5 C). Conversely, in MM samples, CD8+ cells appeared in two distinct clusters, exhibiting PD1 but not TIM3 expression (Figure 5G), with further studies needed to determine their exhaustion status. Finally, by comparing data across platforms, we can identify interactions between macrophages and potentially exhausted T cells (Figure 5D) as well as interactions among various other cell types and differing functional states. The deep sequencing and spatial localization of these cells pave the way for uncovering intricate cellular states. Through mapping the bone tissue microenvironment in diseased conditions, our goal is to highlight potential new therapeutic avenues for MM patients.

References

Janesick, A., Shelansky, R., Gottscho, A.D. *et al.* High resolution mapping of the tumor microenvironment using integrated single-cell, spatial and in situ analysis. *Nat Commun* **14**, 8353 (2023). https://doi.org/10.1038/s41467-023-43458-x

Images and poster were created with BioRender.com